

Article

Enhancing Food Supply Chain in Green Logistics with Multi-Level Processing Strategy under Disruptions

Ming Liu , Hao Tang, Yunfeng Wang *, Ruixi Li, Yi Liu, Xin Liu, Yaqian Wang, Yiyang Wu, Yu Wu and Zhijun Sun

School of Economics & Management, Tongji University, Shanghai 200082, China

* Correspondence: tjuywf@tongji.edu.cn

Abstract: Food supply chains (FSCs) have long been exposed to environmental variability and shock events caused by various economic, political, and infrastructural factors. The outbreak of the COVID-19 pandemic has further exposed and identified the vulnerability of FSCs, and promoted integrated optimization approaches for building resilience. However, existing works focusing on general supply chains (SCs) and FSCs have not been fully aware of the distinct characteristics of FSCs in green logistics, i.e., the expiration of fresh products. In reality, perishable food materials can be processed into products of different processing levels (i.e., multi-level processing) for longer shelf lives, which can serve as a timely and economic strategy to increase safety stocks for mitigating disruption risks. Motivated by this fact, we study the problem of enhancing FSC with a multi-level processing strategy. An integrated location, inventory, and distribution planning model for a multi-echelon FSC under COVID-19-related disruptions is formulated to maximize the total profit over a finite planning horizon. Specifically, a two-stage stochastic programming model is presented to hedge against disruption risks, where scenarios are generated to characterize geographical impact induced by source-region disruptions. For small-scale problems, the model can be solved with commercial solvers. To exactly and efficiently solve the large-scale instances, we design an integer L-shaped method. Numerical experiments are conducted on a case study and randomly generated instances to show the efficiency of our model and solution method. Based on the case study, managerial insights are drawn.



Citation: Liu, M.; Tang, H.; Wang, Y.; Li, R.; Liu, Y.; Liu, X.; Wang, Y.; Wu, Y.; Wu, Y.; Sun, Z. Enhancing Food Supply Chain in Green Logistics with Multi-Level Processing Strategy under Disruptions. *Sustainability* **2023**, *15*, 917. <https://doi.org/10.3390/su15020917>

Academic Editor: Mirco Peron

Received: 12 November 2022

Revised: 23 December 2022

Accepted: 28 December 2022

Published: 4 January 2023



Copyright: © 2023 by the authors. Licensee MDPI, Basel, Switzerland. This article is an open access article distributed under the terms and conditions of the Creative Commons Attribution (CC BY) license (<https://creativecommons.org/licenses/by/4.0/>).

Keywords: COVID-19 related FSC disruption; multi-level processing strategy; two-stage stochastic programming; integer L-shaped method

1. Introduction

In a world of complexity and uncertainty, food supply chains (FSCs) are increasingly threatened by many factors, including multiple slow but major global changes such as climate change, disease outbreaks, pest outbreaks, soil degradation, economic and political crises, and population growth [1]. FSCs of some food products (e.g., seafood) are highly globalized and structurally complex, allowing shocks and disruptions propagation [2]. Almost all parts of FSCs, i.e., food production, storage, processing, distribution, retail, and consumption, are exposed to environmental variability and shock events, which can lead to local disruptions, cascade through FSCs, and finally impact geographically distant places and people. For example, the 2008 drought in the key grain-producing region, along with rising biofuel demand, high oil prices, decreasing grain stocks, and the depreciation of the US dollar, induced price spikes in the global grain market. The disaster further led to a series of rice export bans, shortages, and eventually driving over 130 million people into poverty and an increase of 75 million people into malnourishment [3]. This example embodies the impact of a disruption along the FSC caused by local shocks. Furthermore, the outbreak of the COVID-19 pandemic has also caused disruptions in one country that can have an impact across multiple geographical locations along the SCs [4–7], which is especially unprecedented for FSC.

The disruptions caused by the COVID-19 can lead to differential impacts on food availability (e.g., unharvested fields due to reduced labor), physical and economic access (e.g., restricted movement and transportation, and loss of livelihoods), and intake (e.g., dietary shifts towards highly processed foods with a longer shelf life) [8], which has further exposed and identified the vulnerability of FSCs, and promoted studies on how to build and enhance FSCs to cope with and adapt for future unpredictable shocks [2,9]. To hedge against disruption risks, several typical proactive strategies have been studied for building and improving general SCs under disruption risks, such as (i) multi-sourcing and backup-suppliers [10–15], (ii) pre-positioning of risk mitigation inventory [11,16–18], (iii) nearshoring, shortening global SCs and rebuilding domestic SCs [19], (iv) maintaining ecosystem partnerships with strategic material suppliers (Sarah Hippold, 2020. 6 Strategies for a More Resilient Supply Chain. <https://www.gartner.com/smarterwithgartner/6-strategies-for-a-more-resilient-supply-chain> (accessed on 30 May 2022)). There are also some reactive strategies to mitigate disruption risks (e.g., inventory sharing and customer reallocation [20]). However, due to transportation slowdown during and after the pandemic, the reactive strategies are hard and very costly to apply. Therefore, decision-makers commonly resort to proactive strategies. Furthermore, these strategies designed for general SCs have not fully taken distinct characteristics of FSCs in green logistics into consideration, i.e., expiration of products, which cannot guarantee an uninterrupted supply of food products and, thus, may not be able to achieve resilient FSCs.

Recently, Gholami-Zanjani et al. [21,22,23] considered the troublesome perishability of fresh food products with expiration, and developed a series of integrated location, inventory, and distribution planning models for multi-echelon FSCs and to cope with disruption risks. Specifically, Gholami-Zanjani et al. [21,22] applied both multi-sourcing and backup-suppliers strategies for FSC enhancement; Gholami-Zanjani et al. [23] further took advantage of the capacity-expansion strategy, which is however costly and time-consuming. Moreover, due to the abrupt demands caused by the pandemic together with its geographical complexity, the conflict between perishable food products and such abrupt demands has not been detailedly addressed in these works, which may lead to decreases in safety stocks and increases in the frequency of transportation [24,25]. For example, during the outbreak of the COVID-19 pandemic in Wuhan, JD.COM experienced a critical problem in that demands for food and fresh products increased abruptly owing to the pandemic [26]. Meanwhile, the transportation and operation during lockdown are slowed down, which leads to in-transit and in-stock rotten foods and exacerbates the shortage of fresh food products, as experienced by residents in Shanghai under lockdown (Feiran Lu, 2022. Dumped ‘fresh’ vegetables were actually rotten. Shanghai Daily. <https://www.shine.cn/covid19/220419457\2/> (accessed on 30 May 2022)) To alleviate the supply-demand mismatching condition for fresh products and build a green logistics, this work innovatively proposes a multi-level processing strategy, based on a real-life practice.

In reality, fresh food materials can be processed into products of different processing levels with longer shelf lives, which can help increase safety stocks as a practical risk-mitigating strategy. Apart from risk mitigation, such a multi-level processing strategy is also beneficial for stopping the waste of fresh materials, in contrast to the way of procuring multiple products from multiple suppliers, i.e., multi-sourcing and backup-suppliers strategies. This strategy has important implications for building a food supply chain in green logistics. It has been revealed that food retailers and SCs in high-income countries selling shelf-stable and frozen seafood have done well following COVID-19-related shifts in food sourcing, while live-fresh and high-value producers were particularly hard hit [2,8], since highly processed food products (e.g., frozen products, processed meats, and cans), have lower deterioration rates and can be stored for longer times. Some digital technologies, such as food material freshness detecting and monitoring technologies (e.g., electrical gas sensors [27], computer vision technologies by deep neural network [28]), and inventory level monitoring technologies in a real-time measure (e.g., radio-frequency identification (RFID) [29,30]), facilitate the implementation of multi-level processing strategy.

To fill the gap between existing literature and FSC practice, we study the problem of enhancing FSC with a multi-level processing strategy, where highly processed food products have a lower deterioration rate and, thus, a longer shelf life to cope with disruptions. To portray the FSC under COVID-19-related disruptions, an integrated location, inventory, and distribution planning model under disruptions is formulated. We use different scenarios to characterize uncertain demand, disrupted capacity, and lead time. Specifically, a two-stage stochastic programming model to maximize the total profit is established. To simulate the practice, we specifically portray the geographical spread of disruptions from a source region along the FSC, using the approach from [11]. For solution approaches, we first apply commercial solvers to solve the model for small-scale problems. Then, we design an integer L-shaped method to exactly and efficiently solve the model for large-scale instances. The main contribution of this work can be summarized as follows:

- (1) A new problem of enhancing FSC in green logistics with a multi-level processing strategy is investigated, where food products of different processing levels have distinct deterioration rates and shelf lives;
- (2) An integrated location, inventory, and distribution planning model for a multi-echelon FSC under COVID-19-related disruptions is formulated, where abrupt demand and regional information associated with source region-induced disruption propagations are specifically described via scenarios;
- (3) An exact integer L-shaped method is developed to solve the model efficiently;
- (4) Different deterioration function parameters of food products are investigated in a case study to evaluate the efficiency of a multi-level processing strategy, based on which managerial insights are drawn on whether and when to apply this novel risk-mitigating strategy;
- (5) Numerical experiments are conducted to validate the efficiency of our solution method.

The remainder of this paper is organized as follows. In Section 2, a brief literature review is given. Section 3 states the studied problem, describes the disruption modeling approach, and presents the two-stage stochastic programming model. In Section 4, we present the details of the designed integer L-shaped method. In Section 5, a case study is conducted, and numerical experiments on random instances are conducted. Finally, Section 6 summarizes this paper and suggests future research directions.

2. Literature Review

As new digital technologies arise and become mature to be applied in FSC management, such as electrical gas sensors [27,31], computer vision technologies by deep neural networks [28,32], and RFID [29,30], they provide opportunities for FSCs to improve business performance and adapt for future unpredictable risks. At the same time, the outbreak of the COVID-19 pandemic and other natural or man-made disasters threatening food supply safety have given a boost to studies on FSC [2,8,25]. This section focuses on reviewing the literature on enhancing FSCs under disruption risks, and the most related works on general SCs are also discussed. In the following, we mainly review the applications of operational research methods for SCs with perishable products, which can be distinguished by whether they consider the expiration of products.

2.1. General SC Optimization without Product Expiration

Zahiri et al. [33] studied a multi-objective location and distribution planning problem for a four-echelon pharmaceutical SC, where demand was uncertain under disruptions. With the backup-supplier strategy, the authors proposed a fuzzy optimization approach to deal with uncertainty and developed meta-heuristics to solve the problem. Abbasi et al. [34] investigated a location and distribution planning problem for a four-echelon pharmaceutical SC with multiple perishable products under disruptions. They applied multi-sourcing, fortification, and backup-suppliers strategies to mitigate disruption risks, proposed a bi-objective mixed-integer nonlinear programming model, and developed a fuzzy optimization approach to deal with uncertain capacities caused by disruptions. Diabat

et al. [35] conducted a work on a bi-objective location and distribution planning problem for a four-echelon SC of multiple perishable products under disruptions. The demand and capacity were uncertain in their problem setting. Considering two risk-mitigating strategies, i.e., backup-suppliers and multi-sourcing, they presented a bi-objective robust optimization model and developed a heuristic solution method based on Lagrangian relaxation and ϵ -constraint to solve it. Apart from SCs disruptions, Yavari and Zaker [36] considered power network disruptions in a location and distribution planning problem for a four-echelon SC of multiple perishable products. Risk-mitigating strategies, including backup suppliers, inventory sharing, and capacity-expansion, were considered in their work. The authors proposed a bi-objective stochastic programming model, and applied commercial solvers and LP-metrics method to their model.

Although the above literature considered perishable products, such as pharmaceuticals, they have not taken the expiration of products into consideration. Because for fresh foods, they are easy to deteriorate in a short time. Therefore, a non-ignorable part of the inventory foods may become expired, and demand cannot be satisfied in time, especially during the pandemic. For this reason, the above optimization approaches are not applicable for enhancing FSC under COVID-19 related disruptions.

2.2. FSC Optimization with Product Expiration

Gholami-Zanjani et al. [22] studied a location, inventory, and distribution planning problem for a three-echelon SC with multiple meat products under disruptions, where capacity and demand are uncertain. They considered the expiration of food products, and applied the periodic reorder point and order-up-to-level inventory policy (s, S) . To mitigate disruption risks, the authors adopted backup suppliers and multi-sourcing strategies. A bi-objective two-stage stochastic programming model was presented, and commercial solvers were used to solve it. Gholami-Zanjani et al. [21] also investigated a location, inventory, and distribution planning problem for a three-echelon FSC under disruptions, where capacity, demand are uncertain. The (s, S) inventory policy and multi-sourcing strategy were also applied. They first presented a two-stage stochastic programming model to maximize the total profit, and then adopted a robust optimization technique to obtain solutions. The application of (s, S) inventory policy in Gholami-Zanjani et al. [21,22] leads to mixed-integer second-stage decision variables, which increases computational effort for solvers to obtain solutions, but these two works have not developed exact and efficient algorithms to address this problem. Gholami-Zanjani et al. [23] studied a similar problem but did not consider inventory replenishment decisions. They adopted several different risk-mitigating strategies: backup suppliers, multi-sourcing, and capacity expansion for enhancing the ability of FSC to cope with disruption risks. They also proposed a two-stage stochastic programming model and developed an L-shaped method to solve it. However, all these three works do not apply the easy-to-implement multi-level processing strategy.

Gholami-Zanjani et al. [21] has comprehensively considered FSCs' distinct characteristics (i.e., expiration of food products, and uncertain disrupted capacity and demand), and applied multi-sourcing and backup-suppliers strategies to enhance FSC. Our work extends the study of Gholami-Zanjani et al. [21] in the following aspects: (i) proposing to apply multi-level processing strategy in FSCs to improve its ability in a timely and economic way, which has not been studied in literature; (ii) portraying geographical spread of COVID-19 related disruptions induced by a source region, which is consistent with the reality in China (i.e., the disruptions begin in a source region with high disruption risks and propagate to other regions); (iii) considering uncertain replenishment lead times under disruptions; (iv) designing an integer L-shaped method to exactly and efficiently solve our model since the (s, S) inventory policy leads to mixed-integer second-stage decision variables that cannot be addressed by the classic L-shaped method; (v) drawing managerial insights on whether and when to adopt multi-level processing strategy. The comparison of our work and related literature is presented in Table 1.

Table 1. Comparison of our work and related literature.

Literature	Expiration	Inventory Policy	Disruption Uncertainty			Multi-Sourcing	Backup-Suppliers	Capacity-Expansion	Multi-Level Processing	Source Region-Induced Geographical Spread of Disruptions	Solution Method
			Capacity	Demand	Lead Time						
Zahiri et al. (2017) [33]	-	-	-	✓	-	-	✓	-	-	-	Heuristic
Diabat et al. (2019) [35]	-	-	✓	✓	-	✓	✓	-	-	-	Heuristic Solver
Yavari and Zaker (2020) [36]	-	-	✓	-	-	-	✓	✓	-	-	Solver
Abbasi et al. (2021) [34]	-	-	✓	-	-	✓	✓	-	-	-	Solver
Gholami-Zanjani et al. (2021c) [23]	✓	-	✓	✓	-	✓	✓	✓	-	-	L-shaped
Gholami-Zanjani et al. (2021b) [22]	✓	(s, S)	✓	✓	-	✓	✓	-	-	-	Solver
Gholami-Zanjani et al. (2021a) [21]	✓	(s, S)	✓	✓	-	✓	✓	-	-	-	Solver
This paper	✓	(s, S)	✓	✓	✓	✓	✓	-	✓	✓	Solver, Integer L-shaped

3. Problem Description and Formulation

In this section, we present the details of the integrated location, inventory, and distribution planning problem faced by a single decision-maker under COVID-19-related disruptions, and formulate a two-stage stochastic programming model for it. Specifically, in our problem setting, multi-level processing of food materials, serving as a risk-mitigating strategy for the FSC, is for the first time considered, which distinguishes our work from the related literature [23]. Our unique feature of multi-level processing can significantly enhance FSCs' ability to cope with disruption risks. In Section 3.1, we state the problem and introduce a multi-level processing feature. In Section 3.2, we portray disruptions on a realistic basis. In Section 3.3, a novel two-stage stochastic programming model is presented.

3.1. Problem Description

Considering a three-echelon food supply chain (FSC) consisting of processing centers (PCs) $\mathcal{P} = \{1, 2, \dots, P\}$, distribution centers (DCs) $\mathcal{D} = \{1, 2, \dots, D\}$ and customer zones (CZs) $\mathcal{K} = \{1, 2, \dots, K\}$, which is faced by unforeseen disruption risks under pandemic COVID-19. It focuses on the business of satisfying the food demand of covered CZs, specifically a single type of food demand, such as meat. Customer demand can be satisfied by food products of different processing levels, e.g., fresh meat products and processed meat products, both of which are made of raw meat materials. Food products of different processing levels mainly differ in unit ordering cost, fixed ordering cost, inventory holding cost, transportation cost, replenishment lead time, and shelf life. The food product is ordered and purchased from PCs, stored in the DCs, and transported to CZs to satisfy demand. The storage capacity of PCs and production capacity of DCs is limited. In DCs, a periodic reorder point and order-up-to-level policy (s, S) is applied. At the beginning of each time period, the inventory level of each DC is reviewed using digital technologies such as RFID [29,30], and an order is placed if the inventory level is below the reorder point to replenish the inventory up to the order-up-to level point. When the PCs cannot provide sufficient product due to disruptions, the DCs can replenish inventory by outsourcing from PCs out of the considered FSC at an extra cost. In addition, the throughput capacity of PCs is also considered limited, which describes the maximum quantity of product that can be transported from DCs in a single period. We aim to tactically determine the number of DCs, locations of DCs, the maximum storage and throughput capacity of DCs, and operationally the replenishment (outsourcing) time points and quantities and distribution configurations, to maximize the total profit over a discrete planning horizon $\mathcal{T} = \{1, 2, \dots, T\}$, considering unpredictable pandemic disruptions.

The food product is perishable for all processing levels (i.e., it deteriorates over time), and the freshness of it can be monitored using electrical gas sensors [27,31] or computer vision technologies by deep neural networks [28,32]. Once the product is transported to DCs, its shelf life begins. The products stored in each DC are distinguished by their ages, and the earlier the products are produced, the sooner they are transported to CZs. In this paper, we consider an exponential function $\mu^0 e^{t/\omega}$ [37], where μ^0 is the initial deterioration rate, constant ω denotes the time when the deterioration rate of the product becomes

equal to e times of the initial value. For each processing level l , the fraction μ_{lrt} of product produced in time period r and deteriorated at the end of period t is calculated as follows.

$$\mu_{lrt} = \int_{t-r}^{t-r+1} \mu_l^0 e^{t'/\omega_l} dt' \quad (1)$$

Food products of different processing levels have different deterioration function parameters, which is the essence for adopting multi-level processing strategy to enhance FSC.

The price of food products is usually related to their freshness. In line with Gholami-Zanjani et al. [21], we adopt a linear price function with respect to the product's inventory age as follows.

$$\pi_{lrt} = \pi_l^0 \left(\frac{SL_l - (t-r)}{SL_l} \right), \quad \forall l \in \mathcal{L}, r, t \in \mathcal{T}, r \leq t, \quad (2)$$

where π_l^0 represents the initial price if the product of processing level l is fresh and SL_l denotes the shelf life of processing level l . Different from Gholami-Zanjani et al. [21] that only considered fresh food products, in this paper, food products of different processing levels have different shelf lives SL_l .

3.2. Disruption Modeling

We portray uncertain disruptions, together with their geographical information, in line with Sawik [11]. According to the geographic location and supply chain partnership, supply chain nodes in the FSC are divided into N regions, $\mathcal{N} = \{1, 2, \dots, N\}$. The supply chain nodes in the region $n \in \mathcal{N}$ are denoted by set \mathcal{M}^n . The region $n = 1$ is considered as the source region, which is exposed to regional pandemic disruption risks of different levels $g \in \mathcal{G}_1 = \{0, 1, \dots, G_1\}$, with different probabilities, Pr_{1g} . The disruption levels are characterized by disruption duration, available throughput capacity, replenishment lead time, customer demand, etc. The higher the disruption level, the greater impact it has on business performance. Disruption level 0 refers to normal conditions without disruption. The regional disruption of level $g \in \mathcal{G}_n / \{0\}$ in the source region $n = 1$ can be propagated to other regions $n \in \mathcal{N} / \{1\}$, and trigger disruptions of different levels $g \in \mathcal{G}_n$, with different probabilities Pr_{ng} . Therefore, there is totally $\prod_{n \in \mathcal{N}} (G_n + 1)$ potential scenarios, $\mathcal{S} = \{1, 2, \dots, S = \prod_{n \in \mathcal{N}} (G_n + 1)\}$. Each potential scenario s is represented by a n -dimensional vector $\zeta^s = \{\zeta_{1s}, \zeta_{2s}, \dots, \zeta_{Ns}\}$, where $\zeta_{ns} \in \mathcal{G}_n$ denotes the disruption level in region $n \in \mathcal{N}$ under scenario $s \in \mathcal{S}$. The probability of each potential scenario s is calculated as follows [11].

$$R_s = \prod_{n \in \mathcal{N}} \prod_{g \in \mathcal{G}_n, g = \zeta_{ns}} Pr_{ng}, \quad \forall s \in \mathcal{S} \quad (3)$$

This approach is based on the assumption that, except for the source region, all regions can only be disrupted due to regional disruptions directly propagated from the source region. This assumption simplifies disruption modeling and does not mean loss of generality. It represents the condition faced by a domestic FSC in China where only PCs in the source region have trade contacts with foreign suppliers, and, thus, are exposed to higher pandemic disruption risks, whereas the other regions are not exposed to pandemic disruption risks directly. For example, as the number of confirmed cases was increasing at the outbreak of the COVID-19 pandemic in Germany, China halted imports from German meat plants, which caused disruptions to its meat-import firms (Orange Wang, 2020. Coronavirus: China bans imported pork from German meat plant after more than 650 infected in outbreak. South China Morning Post. <https://www.scmp.com/economy/china-economy/article/3089661/coronavirus-china-bans-imported-pork-german-meat-plant-after> (accessed on 30 May 2022)). Therefore, if the pandemic does not hit the source region, and at least one non-source region has been disrupted, such scenarios are assumed to be infeasible. The probability of these scenarios should be corrected to zero, while the probability of

scenarios where all regions are at normal condition should be augmented to $\sum_{s \in \mathcal{S}, \zeta_{1s}=0} R_s$. The corrected probability $Prob_s$ for each scenario is presented as follows.

$$Prob_s = \begin{cases} \sum_{s' \in \mathcal{S}, \zeta_{1s'}=0} R_{s'} & \text{if } \sum_{n \in \mathcal{N}} \zeta_{ns} = 0 \\ 0 & \text{if } \zeta_{1s} = 0 \text{ and } \sum_{n \in \mathcal{N}/1} \zeta_{ns} > 0 \\ R_s & \text{otherwise} \end{cases} \quad (4)$$

The disruption of each level $g \in \mathcal{G}_1/\{0\}$ in the source region is assumed to occur at the beginning of the planning horizon. Then, with a delay of Λ_{ng} , the disruption of level $g \in \mathcal{G}_n$, begins in region $n \in \mathcal{N}/\{1\}$. The disruption of level $g \in \mathcal{G}_n$ in region $n \in \mathcal{N}$ has a duration of Δ_{ng} . Denoted by Cap_{pl}^0 the production capacity for the product of processing level l in PC p without disruptions in the region $n \in \mathcal{N}$. The production capacity of PCs in the region n under scenario $s \in \mathcal{S}$ is presented as follows.

$$Cap_{plt}^s = \begin{cases} (1 - b_{n\zeta_{ns}})Cap_{pl}^0 & \text{if } \Lambda_{n\zeta_{ns}} < t \leq \Lambda_{n\zeta_{ns}} + \Delta_{ng} \\ Cap_{pl}^0 & \text{otherwise} \end{cases}, \quad (5)$$

where $b_{n\zeta_{ns}} \in [0, 1]$ is the regional capacity reduction factor under disruption level of ζ_{ns} in region n . Likewise, if DC d is established with capacity level $c \in \mathcal{C}$, we use Φ_{dlc}^0 to denote the storage capacity without disruptions in its region. The storage capacity is not impacted by disruptions once it is built, whereas the throughput capacity may decrease due to lockdown. The throughput capacity of DCs in the region $n \in \mathcal{N}$ under scenario $s \in \mathcal{S}$ is given as follows.

$$\Phi_{dlct}^s = \begin{cases} (1 - b_{n\zeta_{ns}})\Phi_{dlc}^0 & \text{if } \Lambda_{n\zeta_{ns}} < t \leq \Lambda_{n\zeta_{ns}} + \Delta_{ng} \\ \Phi_{dlc}^0 & \text{otherwise} \end{cases} \quad (6)$$

When disrupted by pandemic disruptions, replenishment lead time of ordering product from PCs increases due to temporary lockdown and limitation of transportation resources. Denoted by δ_{pl}^0 the replenishment lead time for a product of processing level l from PC p to DCs, if there are no disruptions in its region $n \in \mathcal{N}$. The replenishment lead time δ_{plt}^s under scenario s is expressed as follows,

$$\delta_{plt}^s = \begin{cases} \delta_{pl}^0 + h_{p\zeta_{ns}} & \text{if } \Lambda_{n\zeta_{ns}} < t \leq \Lambda_{n\zeta_{ns}} + \Delta_{ng} \\ \delta_{pl}^0 & \text{otherwise} \end{cases}, \quad (7)$$

where $h_{p\zeta_{ns}}$ represents the replenishment lead time extension under disruption level of ζ_{ns} in region n .

As a distinctive feature of FSC, the demand for food products increases abruptly owing to the pandemic, since the outbreak of disruption in the source region [26]. Influenced by the panic of possible lockdown, customers in both source and non-source regions rush to purchase more food products than normal level. We assume that the demand of each CZ starts to increase since the outbreak of disruption in the source region, and gradually decreases to normal level when its region is disrupted by disruptions propagated from the source region, as depicted in Figure 1. The normal demand level of CZ $k \in \mathcal{K}$ is denoted by q_k^0 , and the maximum demand under scenario $s \in \mathcal{S}$ is impacted by both disruption levels in the source region 1 and the CZ's region n , as $q_{ks}^{max} = v_{\zeta_{1s}n} v_{\zeta_{ns}} q_k^0$, where $v_{\zeta_{1s}n} \geq 1$ represents the impact of regional disruption of level ζ_{1s} in source region 1 on the demand of CZs in region n , and $v_{\zeta_{ns}} \geq 1$ denotes the impact of disruption of level ζ_{ns} in region n on

the demand of CZs in it. The demand q_{kt}^s of CZ k in time period t under scenario $s \in \mathcal{S}$ can, therefore, be expressed as follows.

$$q_{kt}^s = \begin{cases} q_k^0 + \frac{t}{\Lambda_{n\zeta_{ns}}} (q_{ks}^{max} - q_k^0) & \text{if } 1 \leq t < \Lambda_{n\zeta_{ns}} \\ q_{ks}^{max} + \frac{\Lambda_{n\zeta_{ns}} - t}{\Delta_{n\zeta_{ns}}} (q_{ks}^{max} - q_k^0) & \text{if } \Lambda_{n\zeta_{ns}} \leq t < \Lambda_{n\zeta_{ns}} + \Delta_{n\zeta_{ns}} \\ q_k^0 & \text{otherwise} \end{cases} \quad (8)$$

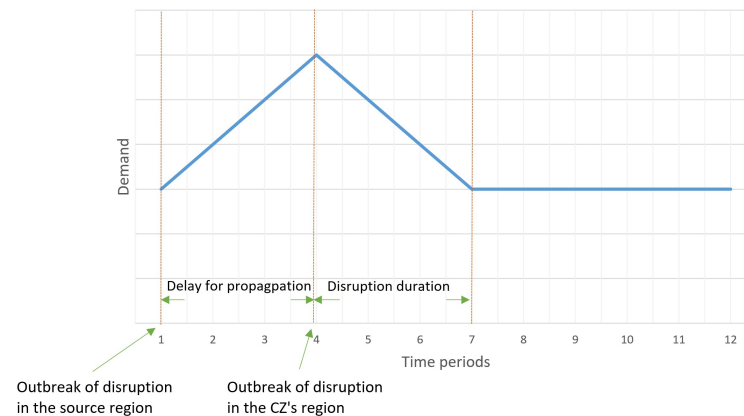


Figure 1. Illustration for demand pattern under pandemic disruption.

3.3. Problem Formulation

In this section, the basic assumptions for problem formulation are given, and the mathematical model for the studied problem is presented.

3.3.1. Problem Assumption

The basic assumptions for problem formulation are concluded and listed as follows.

- (1) The demand for CZs for certain food types can be satisfied by products of all processing levels provided by the FSC, and in this paper, we study two processing levels: fresh and processed. They mainly differ in deterioration function parameters, shelf lives, holding costs, replenishment lead times, and transportation costs;
- (2) Products of different processing levels have distinct shelf lives, storage requirements, replenishment lead times, and per-unit costs and prices;
- (3) Products of different processing levels should be stored in DCs using different equipment, i.e., the capacity for products of different processing levels is independent;
- (4) The transportation time from DCs to CZs is smaller than one time period and can be neglected;
- (5) The supply chain nodes (PCs, DCs and CZs) in a region are faced with identical disruption risks;
- (6) The disruption originates in exactly one source region, occurs at the beginning of the planning horizon, and triggers disruption in the remaining regions with a delay;
- (7) The disruptions propagated from the source region impact the maximum throughput capacity of PCs and DCs, replenishment lead time from PCs to DCs, and demand in CZs;
- (8) The demand of each CZ starts to increase linearly since the outbreak of disruption in the source region, and gradually decreases linearly to normal level when its region is disrupted by disruptions propagated from the source region;
- (9) When the PCs cannot provide sufficient products due to disruptions, DCs can out-source from PCs out of the considered FSC at an extra cost, which is actually the backup-suppliers strategy;

- (10) Backlogging is not allowed, since customers can easily buy other substitute products when their demand cannot be satisfied;
- (11) The deterioration function of food products is an exponential one [37].

3.3.2. The Two-Stage Stochastic Programming Model

The indices and notations for the mathematical model are summarized as follows:

Indices

- t, r, m : index of time periods during the planning horizon;
- i, j : index of nodes in the supply chain network;
- p : index of processing centers (PCs);
- d : index of distribution centers (DCs);
- k : index of customer zones (CZs);
- l : index of processing levels of product;
- c : index of possible capacity levels of DCs;
- g : index of disruption levels;
- s : index of scenarios.

Notations

- \mathcal{T} : set of time periods, $\mathcal{T} = \{1, 2, \dots, T\}$, where T is the length of the planning horizon;
- \mathcal{P} : set of processing centers (PCs), $\mathcal{P} = \{1, 2, \dots, P\}$, where P is the number of PCs;
- \mathcal{D} : set of possible distribution centers (DCs), $\mathcal{D} = \{1, 2, \dots, D\}$, where D is the number of DCs;
- \mathcal{K} : set of possible customer zones (CZs), $\mathcal{K} = \{1, 2, \dots, K\}$, where K is the number of CZs;
- \mathcal{L} : set of possible processing levels, $\mathcal{L} = \{1, 2, \dots, L\}$, where L is the number of processing levels;
- \mathcal{C} : set of possible capacity levels for establishing new DCs, $\mathcal{C} = \{1, 2, \dots, C\}$, where C is the number of processing levels;
- \mathcal{S} : set of scenarios, $\mathcal{S} = \{1, 2, \dots, S\}$, where S is the number of scenarios;
- σ_{dlc} : establishment cost of DC d with capacity level c for product of processed level l , where $d \in \mathcal{D}$, $l \in \mathcal{L}$ and $c \in \mathcal{C}$;
- Cap_{plt}^s : maximum throughput capacity for product of processing level l of PC p in period t under scenario s , where $p \in \mathcal{P}$, $l \in \mathcal{L}$, $t \in \mathcal{T}$ and $s \in \mathcal{S}$;
- Φ_{dlct}^s : maximum throughput capacity for product of processing level l of DC d in period t under scenario s if DC d is established with capacity c for product of processing level l , where Φ_{dlc}^0 represents storage capacity, $d \in \mathcal{D}$, $l \in \mathcal{L}$, $c \in \mathcal{C}$, $t \in \mathcal{T}$ and $s \in \mathcal{S}$;
- τ_{ijl} : transportation cost of per unit product of processing level l from node i to node j , where $l \in \mathcal{L}$ and $i, j \in \mathcal{P} \cup \mathcal{D} \cup \mathcal{K}$;
- SL_l : shelf life for processing level l , where $l \in \mathcal{L}$;
- θ_l : outsourcing cost of per unit product of processing level l , where $l \in \mathcal{L}$;
- α_l : fixed cost of placing an order for product of processing level l , which is independent of the order quantity, where $l \in \mathcal{L}$;
- β_l : procurement cost of per unit product of processing level l from PCs, where $l \in \mathcal{L}$;
- λ_l^+ : holding cost of per unit product of processing level l for one period in DCs, where $l \in \mathcal{L}$;
- λ_l^- : backlogging cost of per unit product of processing level l for one period in DCs, where $l \in \mathcal{L}$;
- π_{lrt} : price of per unit product of processing level l that is produced in period r and sold in period t , where $l \in \mathcal{L}$, $r, t \in \mathcal{T}$ and $r \leq t$;
- μ_{lrt} : fraction of per unit product of processing level l that is produced in period r but becomes expired at the end of period t , where $l \in \mathcal{L}$, $r, t \in \mathcal{T}$ and $r \leq t$;

- ρ_l : deterioration cost of per unit product of processing level l , where $l \in \mathcal{L}$;
 q_{kt}^s : demand of CZ k in period t under scenario s , where $k \in \mathcal{K}$, $t \in \mathcal{T}$ and $s \in \mathcal{S}$;
 δ_{plt}^s : lead time of product of processing level l in PC p that is ordered in period t under scenario s , where $p \in \mathcal{P}$, $l \in \mathcal{L}$, $t \in \mathcal{T}$ and $s \in \mathcal{S}$;
 $Prob_s$: probability of scenario s , where $s \in \mathcal{S}$;
 M : a sufficient large positive number;
 ϵ : a sufficient small positive number.

Decision Variables

- y_d : a binary variable equal to 1 if a DC is established at potential location $d \in \mathcal{D}$; 0, otherwise, $d \in \mathcal{D}$;
 x_{dlc} : a binary variable equal to 1 if a DC is established at potential location d with capacity level c for product of processing level l ; 0, otherwise, where $d \in \mathcal{D}$, $l \in \mathcal{L}$ and $c \in \mathcal{C}$;
 o_{dlt}^s : a binary variable equal to 1 if DC d places an order for product of processing level l at the beginning of period t under scenario s ; 0, otherwise, where $d \in \mathcal{D}$, $l \in \mathcal{L}$, $t \in \mathcal{T}$ and $s \in \mathcal{S}$;
 R_{dl}^s : reorder point of product of processing level l for DC d under scenario s , where $d \in \mathcal{D}$, $l \in \mathcal{L}$ and $s \in \mathcal{S}$;
 U_{dl}^s : up-to-level point of product of processing level l for DC d under scenario s , where $d \in \mathcal{D}$, $l \in \mathcal{L}$ and $s \in \mathcal{S}$;
 w_{dkt}^s : amount of demand of CZ k that is satisfied by DC d in period t under scenario s , where $d \in \mathcal{D}$, $k \in \mathcal{K}$, $t \in \mathcal{T}$ and $s \in \mathcal{S}$;
 b_{dkt}^s : amount of demand of CZ k that should be satisfied by DC d but backlogged till the end of period t under scenario s , where $d \in \mathcal{D}$, $k \in \mathcal{K}$, $t \in \mathcal{T}$ and $s \in \mathcal{S}$. Note that $b_{dk0}^s = 0$ in this paper;
 z_{dklrt}^s : amount of product of processing level l that is produced in period r and transported from DC d to CZ k in period t under scenario s , where $d \in \mathcal{D}$, $k \in \mathcal{K}$, $l \in \mathcal{L}$, $r, t \in \mathcal{T}$, $r \leq t$ and $s \in \mathcal{S}$;
 f_{dplt}^s : amount of product of processing level l transported from PC p to DC d in period t under scenario s , where $d \in \mathcal{D}$, $p \in \mathcal{P}$, $l \in \mathcal{L}$, $t \in \mathcal{T}$ and $s \in \mathcal{S}$;
 I_{dl}^s : inventory position of product of processing level l in DC d at the beginning of period t under scenario s , where $d \in \mathcal{D}$, $l \in \mathcal{L}$, $t \in \mathcal{T}$ and $s \in \mathcal{S}$;
 e_{dlrt}^s : on-hand inventory at the end of period t of product of processing level l in DC d that is produced in period r under scenario s , where $d \in \mathcal{D}$, $l \in \mathcal{L}$, $r, t \in \mathcal{T}$, $r \leq t$, $s \in \mathcal{S}$ and e_{dl00}^s represents the initial inventory (equal to zero in this paper);
 φ_{dlt}^s : outsourcing quantity of product of processing level l in DC d in period t under scenario s , where $d \in \mathcal{D}$, $l \in \mathcal{L}$, $t \in \mathcal{T}$ and $s \in \mathcal{S}$;
 γ_{dlt}^s : order quantity of product of processing level l from DC d in period t under scenario s , where $d \in \mathcal{D}$, $l \in \mathcal{L}$, $t \in \mathcal{T}$ and $s \in \mathcal{S}$.

The two-stage stochastic programming model for the studied problem is detailed below.

$$\max \left\{ \begin{array}{l} - \sum_{d \in \mathcal{D}} \sum_{l \in \mathcal{L}} \sum_{c \in \mathcal{C}} \sigma_{dlc} x_{dlc} - \sum_{p \in \mathcal{P}} \sum_{d \in \mathcal{D}} \eta_{pd} u_{pd} - \sum_{d \in \mathcal{D}} \sum_{k \in \mathcal{K}} \phi_{dk} v_{dk} \\ + \sum_{s \in \mathcal{S}} Prob_s \sum_{d \in \mathcal{D}} \sum_{l \in \mathcal{L}} \sum_{t \in \mathcal{T}} \left(\sum_{k \in \mathcal{K}} \sum_{r \in \mathcal{T}, r \leq t} (\pi_{lrt} - \tau_{dkl}) z_{dklrt}^s - \alpha_l o_{dlt}^s - \beta_l \gamma_{dlt}^s \right) \\ - \sum_{p \in \mathcal{P}} (\beta_l + \tau_{pdl}) f_{dplt}^s - \theta_l \varphi_{dlt}^s - \sum_{r \in \mathcal{T}, r \leq t} (\lambda_l^+ + \rho_l \mu_{lrt}) e_{dlrt}^s - \sum_{k \in \mathcal{K}} \lambda_l^- b_{dkt}^s \end{array} \right\} \quad (9)$$

subject to:

$$\sum_{c \in \mathcal{C}} x_{dlc} \leq y_d, \quad \forall d \in \mathcal{D}, l \in \mathcal{L} \quad (10)$$

$$\sum_{l \in \mathcal{L}} \sum_{c \in \mathcal{C}} x_{dlc} \geq y_d, \quad \forall d \in \mathcal{D} \quad (11)$$

$$\sum_{d \in \mathcal{D}} w_{dkt}^s \leq q_{kt}^s, \quad \forall k \in \mathcal{K}, t \in \mathcal{T}, s \in \mathcal{S} \quad (12)$$

$$w_{dkt}^s + b_{dk,t-1}^s = \sum_{l \in \mathcal{L}} \sum_{r \in \mathcal{T}, r \leq t} z_{dklrt}^s + b_{dkt}^s, \quad \forall d \in \mathcal{D}, k \in \mathcal{K}, t \in \mathcal{T}, s \in \mathcal{S} \quad (13)$$

$$b_{dkT}^s = 0, \quad \forall d \in \mathcal{D}, k \in \mathcal{K}, s \in \mathcal{S} \quad (14)$$

$$I_{dlt}^s = \sum_{r \in \mathcal{T}, t - SL_l + 1 \leq r \leq t - 1} (1 - \mu_{lrt-1}) e_{dlr,t-1}^s + \sum_{p \in \mathcal{P}} \sum_{r=t}^{t+\delta_{plt}^s} f_{dplr}^s, \quad \forall d \in \mathcal{D}, l \in \mathcal{L}, t \in \mathcal{T}, s \in \mathcal{S} \quad (15)$$

$$e_{dlrt}^s = \sum_{p \in \mathcal{P}} f_{dplt}^s + \varphi_{dlt}^s - \sum_{k \in \mathcal{K}} z_{dklrt}^s, \quad \forall d \in \mathcal{D}, l \in \mathcal{L}, r, t \in \mathcal{T}, r = t, s \in \mathcal{S} \quad (16)$$

$$(1 - \mu_{lrt-1}) e_{dlr,t-1}^s = e_{dlrt}^s + \sum_{k \in \mathcal{K}} z_{dklrt}^s, \quad \forall d \in \mathcal{D}, l \in \mathcal{L}, r, t \in \mathcal{T}, r < t \leq r + SL_l - 1, s \in \mathcal{S} \quad (17)$$

$$I_{dlt}^s \leq R_{dl}^s - \epsilon + M(1 - o_{dlt}^s), \quad \forall d \in \mathcal{D}, l \in \mathcal{L}, t \in \mathcal{T}, s \in \mathcal{S} \quad (18)$$

$$I_{dlt}^s \geq R_{dl}^s - Mo_{dlt}^s, \quad \forall d \in \mathcal{D}, l \in \mathcal{L}, t \in \mathcal{T}, s \in \mathcal{S} \quad (19)$$

$$o_{dlt}^s \leq \sum_{c \in \mathcal{C}} x_{dlc}, \quad \forall d \in \mathcal{D}, l \in \mathcal{L}, t \in \mathcal{T}, s \in \mathcal{S} \quad (20)$$

$$\gamma_{dlt}^s \geq U_{dl}^s - I_{dlt}^s - M(1 - o_{dlt}^s), \quad \forall d \in \mathcal{D}, l \in \mathcal{L}, t \in \mathcal{T}, s \in \mathcal{S} \quad (21)$$

$$\gamma_{dlt}^s \leq U_{dl}^s - I_{dlt}^s, \quad \forall d \in \mathcal{D}, l \in \mathcal{L}, t \in \mathcal{T}, s \in \mathcal{S} \quad (22)$$

$$\gamma_{dlt}^s \leq Mo_{dlt}^s, \quad \forall d \in \mathcal{D}, l \in \mathcal{L}, t \in \mathcal{T}, s \in \mathcal{S} \quad (23)$$

$$\gamma_{dlt}^s = \sum_{p \in \mathcal{P}} \sum_{r=t+\delta_{plt}^s} f_{dplr}^s, \quad \forall d \in \mathcal{D}, l \in \mathcal{L}, t \in \mathcal{T}, s \in \mathcal{S} \quad (24)$$

$$\sum_{d \in \mathcal{D}} f_{dplt}^s \leq Cap_{plt}^s, \quad \forall p \in \mathcal{P}, l \in \mathcal{L}, t \in \mathcal{T}, s \in \mathcal{S} \quad (25)$$

$$\sum_{k \in \mathcal{K}} \sum_{r \in \mathcal{T}, r \leq t} z_{dklrt}^s \leq \sum_{c \in \mathcal{C}} \Phi_{dlct}^s x_{dlc}, \quad \forall d \in \mathcal{D}, l \in \mathcal{L}, t \in \mathcal{T}, s \in \mathcal{S} \quad (26)$$

$$\sum_{r \in \mathcal{T}, r \leq t} e_{dlrt}^s \leq \sum_{c \in \mathcal{C}} \Phi_{dlc}^0 x_{dlc}, \quad \forall d \in \mathcal{D}, l \in \mathcal{L}, t \in \mathcal{T}, s \in \mathcal{S} \quad (27)$$

$$y_d, x_{dlc}, o_{dlt}^s \in \{0, 1\}, \quad \forall p \in \mathcal{P}, d \in \mathcal{D}, k \in \mathcal{K}, c \in \mathcal{C}, l \in \mathcal{L}, t \in \mathcal{T}, s \in \mathcal{S} \quad (28)$$

$$R_{dl}, U_{dl}, w_{dkt}^s, z_{dklrt}^s, f_{dplt}^s, I_{dlt}^s, e_{dlrt}^s, \varphi_{dlt}^s, \gamma_{dlt}^s \geq 0, \quad \forall d \in \mathcal{D}, d \in \mathcal{D}, k \in \mathcal{K}, l \in \mathcal{L}, r, t \in \mathcal{T}, r \leq t, s \in \mathcal{S} \quad (29)$$

The objective function of maximizing the total profit is given by (9), which includes establishment costs of DCs in the first-stage decision, and revenue of satisfying customer demand, the procurement costs of DCs, the fixed ordering costs of DCs, outsourcing cost of DCs, the transportation costs, the inventory holding costs and deterioration costs in second-stage decision.

The constraints related to the first-stage decision are given by (10) and (11). Constraints (10) ensure that at most one DC is established at a potential location and each DC is established with a capacity level for the product of each processing level. Constraints (11) state that if one DC is established at a potential location, it should be built up for at least one processing level.

The constraints related to the second-stage decision are stated by (12)–(27). Constraints (12) mean that the supply for each CZ cannot exceed its maximum demand. The backloging flow conservation is described by Constraints (13). The demand of each CZ can be satisfied by the product of all processing levels, as stated by Constraints (13). Constraints (11) ensure that the backloged demand is equal to zero at the end of the

planning horizon. Constraints (15) calculate the inventory position for the product of each processing level in each DC at the beginning of each period, which includes on-hand and in-transit inventory. Constraints (16) and (17) represent the inventory material flow conservation constraints. Constraints (18) and (19) mean that DCs places an order if and only if their inventory positions are less than or equal to reorder points at the beginning of each time period. Constraints (20) ensure that orders can only be placed by established DCs. Constraints (21)–(23) calculate order quantities if an order is placed for each DC. Constraints (24) calculate the transportation quantities considering lead time. The maximum production capacity constraints for PCs are described by (25), while the throughput capacity constraints for DCs are described by (26). Constraints (27) ensure that the inventory level in DCs for the product of each processing level at the end of each period should be less or equal to the maximum storage capacity. The domains of decision variables are given by (28) and (29).

4. Solution Method

The proposed mathematical formulation is a two-stage stochastic programming model, which includes purely binary first-stage decision variables and mixed-integer second-stage decision variables. For small-scale problems, we can resort to commercial solvers for solutions. However, the model is fairly intractable as the number of scenarios increases for convergence of the sample average approximation method. To tackle this problem, we design an integer L-shaped method that could reduce the computational effort for evaluating the second stage objective function value. This approach is developed by [38] and latter improved by [39]. In the following subsections, we present the decomposed matrix form of the two-stage stochastic programming model and provide the details of our algorithm.

4.1. Decomposition

The original two-stage stochastic programming model is decomposed into a master problem (MP) with binary decision variables and S subproblems (SPs) with mixed-integer decision variables, where S represents the number of scenarios [40]. In this subsection, the matrix forms of the original model, and decomposed MP and SPs are presented.

The first-stage decision variables are first divided into two categories: Z and V according to whether they are directly related to second-stage constraints. The second-stage decision variables for scenario s are divided into two categories: X_s for binary variables, and Y_s for continuous variables. The first-stage decision variables in the mathematical model can be represented by vectors, such as y for y_d , and x for x_{dlc} . According to the two-stage stochastic programming model, Z includes variables y_d and V includes variables x_{dlc} . Among second stage decision variables, only o_{dlc}^s is binary. Therefore, X_s only includes variable o_{dlc}^s . The matrix form of the original two-stage stochastic model is presented as follows.

$$\max \left\{ c_z Z + c_v V + \sum_{s \in S} Prob_s (c_x^s X_s + c_y^s Y_s) \right\} \quad (30)$$

subject to:

$$AZ + BV \leq b \quad (31)$$

$$W_x^s X_s + W_y^s Y_s = h_s - T_v^s V, \quad \forall s \in S \quad (32)$$

$$Z \in \{0, 1\}^{m_z}, V \in \{0, 1\}^{m_v}, X_s \in \{0, 1\}^{m_x}, Y_s \in \mathbb{R}_+^{m_y}, \quad \forall s \in S \quad (33)$$

where c_z , c_v , c_x^s , and c_y^s are corresponding coefficient vectors of decision variables, matrix A and B are obtained from Constraints (10) and (11), and b represents the right-hand side constant vector of Constraints (10) and (11). In (32), W_y^s and W_x^s represent the recourse matrices corresponding to X_s and Y_s , T_v^s is the technology matrices corresponding to

V , and h_s denotes the resource vectors. Constraints (33) states the domains of decision variables, where m_z , m_v , m_x , and m_y are the size of corresponding vectors.

The second-stage objective function is represented by $Q(V)$. By introducing an auxiliary variable η , the master problem (MP) is formulated as follows.

$$[\text{MP}] \quad \max F_{\text{MP}} = c_z Z + c_v V + \eta \quad (34)$$

subject to:

$$AZ + BV \leq b \quad (35)$$

$$\eta \leq \bar{\eta} \quad (36)$$

$$Z \in \{0, 1\}^{m_z}, V \in \{0, 1\}^{m_v} \quad (37)$$

where $\bar{\eta}$ is an upper bound of $Q(V)$ to avoid unboundedness of the problem, and it can be obtained by assuming DCs are established at all potential locations with sufficient capacity. The solution of MP provides an upper bound for the original two-stage stochastic programming model. For any given solution \bar{Z} and \bar{V} , the subproblem (SP_s) for scenario s can be formulated as follows.

$$[\text{SP}_s] \quad \max F_{\text{SP}_s} = c_x^s X_s + c_y^s Y_s \quad (38)$$

subject to:

$$W_x^s X_s + W_y^s Y_s = h_s - T_v^s \bar{V} \quad (39)$$

$$X_s \in \{0, 1\}^{m_x}, Y_s \in \mathbb{R}_+^{m_y} \quad (40)$$

4.2. Integer L-Shaped Method

The classic L-shaped method is developed by [41] for solving a two-stage stochastic programming model where second-stage subproblems are linear programs (LPs). However, when the second-stage decision includes mixed-integer variables, optimality cuts, and feasibility cuts cannot be obtained by using LP duality. The integer L-shaped optimality cut is introduced by [38] for two-stage stochastic programming with binary second-stage variables as follows (it is described in the form for maximum problem).

$$\eta \leq (Q(V^i) - U) \left(\sum_{j \in \mathcal{O}(V^i)} x_j - \sum_{j \notin \mathcal{O}(V^i)} x_j - |\mathcal{O}(V^i)| \right) + Q(V^i) \quad (41)$$

where $Q(V^i)$ denotes the second-stage objective function value in iteration i of the algorithm, U is an upper bound for $Q(V)$, and $\mathcal{O}(V^i)$ is the set of indices for second-stage binary variables that take the value of 1 in iteration i . As mentioned before, the upper bound U can be obtained by assuming that DCs are established at all potential locations with sufficient capacity. The optimality cut can be added to the MP to ensure that $\eta \leq Q(V^i)$ for the first-stage solution V^i , whereas this optimality cut is not tight for other first-stage solutions. Ref. [38] combine the integer L-shaped optimality cut and branch-and-bound scheme for the master problem. On each node of the branch-and-bound tree of the master problem, the values of some first-stage decision variables are fixed, and the master problem is solved based on these fixed values. When a solution at a node is obtained, the integrality of the first-stage decision variables is first checked. If the solution satisfies integrality restriction, the algorithm further checks whether $\eta \geq Q(V^i)$. If this condition is not satisfied, an integer L-shaped optimality cut of form (41) is added to the master problem. In their algorithm, exact evaluation for the value of $Q(V^i)$ is required every time a feasible first-stage solution is obtained. It may be much more time-consuming since the mixed-integer subproblem for each scenario should be solved. Ref. [39] improve the algorithm by using the information on linear relaxation of mixed-integer subproblems. The objective function of LP relaxation is denoted by $Q_{LP}(V^i)$. For maximum subproblems, the condition $Q_{LP}(V^i) \geq Q(V^i)$ holds

on, therefore, the algorithm can be improved by first checking whether $\eta > Q_{LP}(V^i)$. If this condition holds on, the computational effort of evaluating the objective function value of mixed-integer subproblems can be reduced. The solution can be removed by adding continuous L-shaped optimality cut into a master problem using duality information of subproblem LP relaxation as follows:

$$\eta \geq \sum_{s \in \mathcal{S}} Prob_s \pi_i^{s'} h_s - \sum_{s \in \mathcal{S}} Prob_s \pi_i^{s'} T_v^s V, \quad (42)$$

where π_i^s is optimal dual variables of LP relaxation of the subproblem under scenario s in iteration i .

Refs. [38,39] implement the L-shaped method along with branch-and-bound scheme for solving the master problem, whereas in this paper, we simplify the implementation by using a commercial solver to address the master problem since our master problem is not very complicated. By now, we can present the main steps of our implementation as follows:

- Step 0: Let $i = 0$ denote the number of iterations, and define $LB = -inf$ and $UB = inf$ as the lower bound and upper bound of the original two-stage stochastic programming model, respectively.
- Step 1: Solve the MP, obtain optimal solution (Z^i, V^i, η^i) , update UB as the obtained objective function value F_{MP}^i and set $i = i + 1$. If $UB - LB \leq \epsilon$, stop. Otherwise, go to Step 2.
- Step 2: Solve the LP relaxation of each subproblem for $s \in \mathcal{S}$. If $\eta^i > Q_{LP}(V^i)$, add continuous L-shaped optimality cut of form (42) and return to Step 1. Otherwise, go to Step 3.
- Step 3: Solve the subproblems for $s \in \mathcal{S}$. If $F_{MP}^i - \eta + Q(V^i) > LB$, update LB , add integer L-shaped optimality cut of form (41) into the master problem and return to Step 1. Otherwise, stop.

Note that the procedure of adding feasibility cuts into the master problem is omitted since our second-stage subproblems are always feasible.

5. Numerical Experiment

In this section, we first investigate the efficiency of applying the new multi-level processing strategy for FSCs under COVID-19-related disruptions through a case study. Based on the case study, we draw managerial insights on whether and when to apply this novel risk-mitigating strategy. To evaluate the efficiency of our integer L-shaped method, we conduct numerical experiments on randomly generated instances and compare the results with commercial solver.

5.1. Case Study

In this subsection, we present an example of an FSC under source region-induced disruption in China, which includes 3 regions, 2 PCs, 5 potential DCs, and 5 CZs, and the integrated location, inventory, and distribution decisions should be made for a planning horizon with 12 periods, as depicted in Figure 2. Different deterioration function parameters and disruption levels are investigated to evaluate the efficiency of applying a multi-level processing strategy.

The parameters of the example used in the case study are provided in Tables 2 and 3. We consider two processing levels in the example, i.e., fresh meat and highly processed meat. They mainly differ in deterioration function parameters, shelf lives, holding costs, replenishment lead times, and transportation costs. In reality, the demands for food products cannot be backlogged, since customers can easily buy other substitute foods; therefore, the backlogging costs are set to be sufficiently large. By the scenario-related parameters in Table 3, a total of 19 scenarios are generated using the disruption modeling approach detailed in Section 3.2.

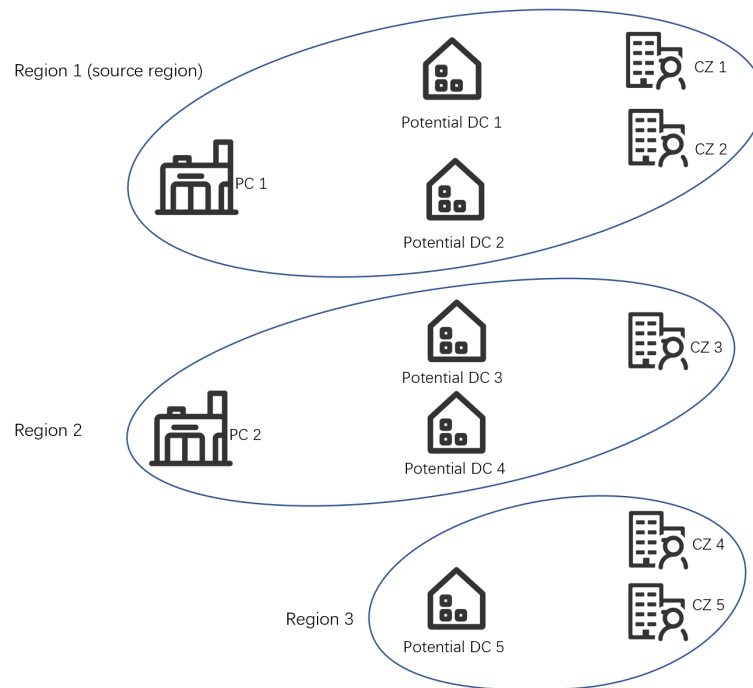


Figure 2. Example used in the case study.

Table 2. Basic parameters of the example.

Instance Scale:	
$N = 3$ (3 regions), $P = 2$ (2 PCs), $D = 5$ (5 potential DCs), $K = 5$ (5 CZs), $T = 12$ (12 periods)	
$L = 2$ (2 processing levels), $C = 3$ (3 capacity levels for DCs), $G_n = 3$ (3 disruption levels for each region)	
Parameters related to PCs:	
Normal production capacity	$Cap_{p1}^0 = 6000, Cap_{p2}^0 = 6000, Cap_{p3}^0 = 5000, Cap_{p4}^0 = 5000$
Normal lead time	$\delta_{p1}^0 = 0, \delta_{p2}^0 = 0, \forall p \in \mathcal{P}$
Parameters related to DCs:	
Normal storage capacity	$\Phi_{d11}^0 = 2000, \Phi_{d12}^0 = 4000, \Phi_{d13}^0 = 6000, \forall d \in \mathcal{D}, l \in \mathcal{L}$
Establishment cost	$\sigma_{d11} = 10000, \sigma_{d12} = 16000, \sigma_{d13} = 20000, \forall d \in \mathcal{D}$
	$\sigma_{d21} = 5000, \sigma_{d22} = 8000, \sigma_{d23} = 10000, \forall d \in \mathcal{D}$
Parameters related to CZs:	
Normal demand	$q_1^0 = 400, q_2^0 = 350, q_3^0 = 420, q_4^0 = 370, q_5^0 = 440$
Transportation cost:	
From PCs to DCs	$\tau_{ij1} \in (2, 3), \forall i \in \mathcal{P}, j \in \mathcal{D}, \tau_{ij2} \in (0, 1), \forall i \in \mathcal{P}, j \in \mathcal{D}$
From DCs to CZs	$\tau_{ij1} \in (1, 2), \forall i \in \mathcal{D}, j \in \mathcal{K}, \tau_{ij2} \in (0, 1), \forall i \in \mathcal{D}, j \in \mathcal{K}$
Parameters related to different processing levels:	
Fresh price	$\pi_1^0 = 35, \pi_2^0 = 37$
Ordering cost	$\beta_1 = 12, \beta_2 = 20$
Fixed ordering cost	$\alpha_1 = 500, \alpha_2 = 500$
Outsourcing cost	$\theta_1 = 35, \theta_2 = 37$
Shelf life	$SL_1 = 4, SL_2 = 12$
Inventory holding cost	$\lambda_1^+ = 0.5, \lambda_2^+ = 0.2$
Backlogging cost	Sufficient large
Deterioration cost	$\rho_1 = 1.5, \rho_2 = 1$
Deterioration function parameter	$\mu_1^0 = 0.03, \mu_2^0 = 0.01$
	$\omega_1 = 4, \omega_2 = 12$

Table 3. Scenario-related parameters for the example.

Parameters	Region	Disruption Level		
		Normal	Partly Disrupted	Disrupted
Disruption probability Pr_{ng}	1	0.3	0.5	0.2
	2	0.5	0.3	0.2
	3	0.6	0.3	0.1
Capacity reduction factor $b_{n\zeta_{ns}}$	1	0	0.7	1
	2	0	0.5	1
	3	0	0.5	1
Delay of regional disruption Λ_{ng}	1	0	0	0
	2	0	2	1
	3	0	3	1
Duration of disruption Δ_{ng}	1	0	4	8
	2	0	3	6
	3	0	3	6
Lead time extension for PCs $h_{p\zeta_{ns}}$	1	0	1	3
	2	0	1	2
	3	0	1	2
Demand impact factor $v_{\zeta_{1s}n}$	1	1	1.25	1.5
	2	1	1.1	1.2
	3	1	1.05	1.15
Demand impact factor $v_{\zeta_{ns}}$	1	1	1	1
	2	1	1.2	1.3
	3	1	1.2	1.4

We focus on 3 indicators: objective function value, expected demand fulfillment rate of all CZs (which is calculated by $\sum_{s \in S} Prob_s \frac{\text{Satisfied_demand}}{\text{Total_demand}} \times 100\%$), and expected rate of demand that is satisfied by fresh meat (which is calculated by $\sum_{s \in S} Prob_s \frac{\text{Demand_satisfied_by_fresh_meat}}{\text{Satisfied_demand}} \times 100\%$).

The objective function value for the example is 108,497.89, where potential DC 1 is established for storing processed meat, potential DC 4 for both fresh meat and processed meat, and potential DC 5 for processed meat. Potential DC 2 and DC 3 are not established. For all 19 different scenarios, the expected demand fulfillment rate of all CZs is 38.61%, of which 32.10% is satisfied by fresh meat and 67.90% is satisfied by processed meat.

To further investigate the efficiency of applying a multi-level processing strategy, we solve the example without considering a multi-level processing strategy, i.e., the FSC only provides fresh meat. To achieve a fair comparison, we set the production capacity of PCS for supplying meat to be 12,000 and 10,000 in PC 1 and 2, capacity levels of DCs to be 4000, 8000, and 120,000, and the corresponding establishment costs to be 20,000, 320,000, and 400,000, respectively. The objective function value obtained is 77,579.76 and the expected demand fulfillment rate is 27.31%, which are smaller than that of considering a multi-level processing strategy. The result shows that a multi-level processing strategy can help improve the total profit and demand fulfillment rate for the FSC under disruptions.

We also investigate whether the multi-level processing strategy is always beneficial. In our original example, the fresh meat is easy to deteriorate while processed meat can hardly expire in the planning horizon. We vary the deterioration function parameters μ_2^0 and ω_2 , and shelf life SL_2 to investigate other situations where two processing levels may be similar. Five combinations of $(\mu_2^0, \omega_2, SL_2)$ are tested, including (0.01, 12, 12), (0.015, 10, 10), (0.02, 8, 8), (0.025, 6, 6), and (0.03, 4, 4), where the combination 1 represents that food product of processing level 2 is not easy to deteriorate, while the combination 5 denotes that food product of processing level 2 are more easy to deteriorate. The obtained results are depicted in Figure 3. As we can see from the figure, both the objective function value and expected demand fulfillment rate decrease as the food product of processing

level 2 become more perishable. Note that the expected demand fulfillment rate under combination 5 is 21.22%, which is smaller than that of not applying a multi-level processing strategy. It means that as two processing levels are more similar, i.e., food products of two processing levels have similar deterioration function parameters, the efficiency of the multi-level processing strategy decreases.

We can conclude the managerial insight obtained from the case study: (i) for FSCs with fresh food products that are easy to deteriorate and expire, such as fresh meat, a multi-level processing strategy can help improve the total profit, and demand fulfillment rate for FSC under source region-induced disruptions; (ii) the efficiency of multi-level processing strategy decreases as food products of two processing levels have similar deterioration function parameters.

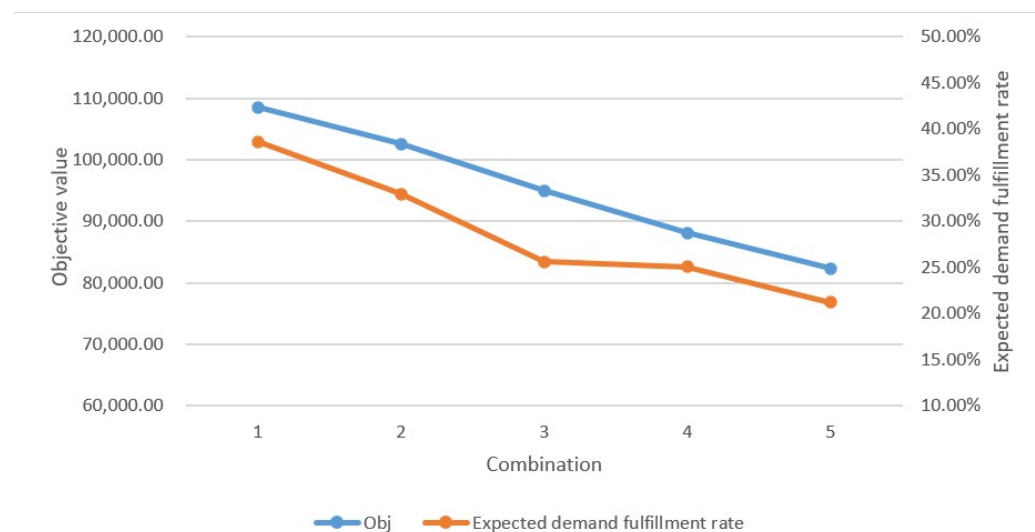


Figure 3. The obtained results for five combinations of parameters.

5.2. Numerical Result on Randomly Generated Instance

In this subsection, we compare the efficiency of our solution method with the state-of-art commercial solver Gurobi of version 9.1.2. In the implementation of our integer L-shaped method, we use Gurobi to solve the master problem, the mixed-integer subproblems, and the LP relaxation of subproblems. The integer L-shaped method is coded in Python and the Gurobi 9.1.2 is also called in Python to solve the two-stage stochastic programming model with a time limit of 3600 s. All the experiments are conducted on a personal computer with 2.4 GHz Intel Core i5 and 16 GB RAM.

5.2.1. Instance Generation

The randomly generated instances used in numerical experiments can be classified into three sets according to the number of regions and the number of nodes in the FSC, as in Table 4. As in the case study, 12 periods, 2 processing levels, 3 capacity levels for DCs, and 3 disruption levels are considered for each region in the randomly generated instances, i.e., normal, partly disrupted, and disrupted. For each instance set, we generate 5 instances.

Table 4. The instance sets used in numerical experiments.

Instance Set	Number of Regions	Number of PCs	Number of DCs	Number of CZs
1	3	2	5	5
2	3	3	10	10
3	4	4	15	15

The instances are generated according to the ranges provided in Tables 5 and 6. Note that the generated disruption probabilities for each region are normalized.

Table 5. Basic parameter ranges for generating instances.

Parameters related to PCs:	
Normal production capacity	$Cap_{pl}^0 \in [4000, 10000], \forall p \in \mathcal{P}, l \in \mathcal{L}$
Normal lead time	$\delta_{pl}^0 = 0, \forall p \in \mathcal{P}, l \in \mathcal{L}$
Parameters related to DCs:	
Normal storage capacity	$\Phi_{dlc}^0 \in [1000, 7000], \forall d \in \mathcal{D}, l \in \mathcal{L}, c \in \mathcal{C}$
Establishment cost	$\sigma_{d1c} = 2\Phi_{dlc}^0, \sigma_{d2c} = 1.5\Phi_{dlc}^0, \forall d \in \mathcal{D}, c \in \mathcal{C}$
Parameters related to CZs:	
Normal demand	$q_k^0 \in [300, 500], \forall k \in \mathcal{K}$
Transportation cost:	
From PCs to DCs	$\tau_{ij1} \in (2, 3), \forall i \in \mathcal{P}, j \in \mathcal{D}, \tau_{ij2} \in (0, 1), \forall i \in \mathcal{P}, j \in \mathcal{D}$
From DCs to CZs	$\tau_{ij1} \in (1, 2), \forall i \in \mathcal{D}, j \in \mathcal{K}, \tau_{ij2} \in (0, 1), \forall i \in \mathcal{D}, j \in \mathcal{K}$
Parameters related to different processing levels:	
Fresh price	$\pi_1^0 = 35, \pi_2^0 = 37$
Ordering cost	$\beta_1 = 12, \beta_2 = 20$
Fixed ordering cost	$\alpha_1 = 500, \alpha_2 = 500$
Outsourcing cost	$\theta_1 = 35, \theta_2 = 37$
Shelf life	$SL_1 = 4, SL_2 = 12$
Inventory holding cost	$\lambda_1^+ = 0.5, \lambda_2^+ = 0.2$
Backlogging cost	Sufficient large
Deterioration cost	$\rho_1 = 1.5, \rho_2 = 1$
Deterioration function parameter	$\mu_1^0 = 0.03, \mu_2^0 = 0.01$
	$\omega_1 = 4, \omega_2 = 12$

Table 6. Scenario-related parameter ranges for generating instances.

Parameters	Region	Disruption Level		
		Normal	Partly Disrupted	Disrupted
Disruption probability Pr_{ng}	1	[0.3, 0.5]	[0.4, 0.6]	[0.1, 0.3]
	Other	[0.5, 0.8]	[0.2, 0.3]	(0, 0.1)
Capacity reduction factor $b_{n\zeta_{ns}}$	1	0	[0.5, 0.8]	[0.9, 1]
	Other	0	[0.4, 0.7]	[0.9, 1]
Delay of regional disruption Λ_{ng}	1	0	0	0
	Other	0	[1, 2]	1
Duration of disruption Δ_{ng}	1	0	[3, 5]	[5, 8]
	Other	0	[1, 3]	[3, 5]
Lead time extension for PCs $h_{p\zeta_{ns}}$	1	0	1	2
	Other	0	1	2
Demand impact factor $v_{\zeta_{1s}n}$	1	1	[1.15, 1.25]	[1.25, 1.5]
	Other	1	[1.05, 1.15]	[1.15, 1.25]
Demand impact factor $v_{\zeta_{ns}}$	1	1	1	1
	Other	1	[1.15, 1.25]	[1.25, 1.5]

5.2.2. Numerical Experiment Result Comparison

In this subsection, the results of numerical experiments are presented and compared. For the commercial solver Gurobi, five indicators are reported, including the objective function value of the best solution found in 3600 s (Obj_g), the best upper bound found by the solver (Obj_bound), the computational time (Time), and the gap to best upper bound ($Gap_b^g = \frac{Obj_bound - Obj_g}{Obj_bound} \times 100\%$). For the integer L-shaped method, we record four indicators, including objective function value (Obj_l), the computational time (Time), an improvement

compared to the best objective function value found by Gurobi ($\text{Imp}_l = \frac{\text{Obj}_l - \text{Obj}_g}{\text{Obj}_g} \times \%$), and gap to the best upper bound found by Gurobi ($\text{Gap}_b^l = \frac{\text{Obj_bound} - \text{Obj}_l}{\text{Obj_bound}} \times \%$). The results of numerical experiments are provided in Table 7.

Table 7. Numerical experiment results.

Instance Set	Instance	Gurobi				Integer L-Shaped Method			
		Obj	Obj_bound	Time	Gap _b ^g	Obj	Time	Imp _l	Gap _b ^l
1	1	129,554.67	129,554.67	71.92	0.00%	129,554.67	38.09	0.00%	0.00%
	2	155,232.48	155,232.48	68.31	0.00%	155,232.48	23.42	0.00%	0.00%
	3	150,420.27	150,420.27	95.98	0.00%	150,420.27	26.49	0.00%	0.00%
2	1	300,345.75	306,162.32	3600.00	1.90%	302,143.44	3600.00	0.60%	1.31%
	2	275,639.19	299,357.20	3600.00	7.92%	279,718.31	3600.00	1.48%	6.56%
	3	322,675.30	337,239.50	3600.00	4.32%	322,963.57	3600.00	0.09%	4.23%
3	1	326,753.97	358,818.78	3600.00	8.94%	329,763.85	3600.00	0.92%	8.10%
	2	250,384.65	287,815.14	3600.00	13.01%	260,751.93	3600.00	4.14%	9.40%
	3	332,955.47	354,903.64	3600.00	6.18%	338,607.20	3600.00	1.70%	4.59%

It can be observed from the results that both the solver and integer L-shaped method can obtain optimal solutions, for instance, set 1, but the latter is more efficient in terms of computational times. As the problem size increases, the computational times of both solution methods increase significantly. Although both solution methods cannot yield optimal solutions within 3600 s, for instance, sets 2 and 3, we can see that the integer L-shaped method can find better feasible solutions. The numerical experiments validate the efficiency of our integer L-shaped method.

6. Conclusions and Future Research

In this paper, we study a new problem of enhancing FSC with a multi-level processing strategy under COVID-19-related disruptions. An integrated location, inventory, and distribution planning model is formulated to portray the FSC under the geographical spread of disruptions, where scenarios are generated to characterize uncertain demand, capacity, and lead time, as well as the geographical spread of disruptions induced by a source region. Specifically, a two-stage stochastic programming model to maximize the total profit is presented, which can be solved via a commercial solver for small-scale problems. To exactly and efficiently solve the model for large-scale instances, we design an integer L-shaped method. We conduct a case study to illustrate the efficiency of applying a multi-level processing strategy and draw managerial insights. Numerical experiments on randomly generated instances are performed to show the efficiency of the designed solution method.

Future research directions may include: (i) developing efficient heuristic to obtain near-optimal solutions in fewer times, which can also be used to generate better initial lower bound for the integer L-shaped method; (ii) considering customer satisfaction as customers, in reality, have different satisfaction degrees on food products of different processing levels, and multi-objective optimization approach should be developed; (iii) investigating another advantage of multi-level processing, i.e., process flexibility, as it can further enhance FSC and reduce waste of foods.

Author Contributions: Conceptualization, M.L.; methodology, H.T.; software, Y.W. (Yaqian Wang); validation, H.T.; investigation, Y.L. and Y.W. (Yu Wu); data curation, R.L.; writing—original draft, H.T.; writing—review and editing, M.L., R.L., Y.L., X.L., Y.W. (Yaqian Wang), Y.W. (Yiyang Wu), Y.W. (Yu Wu), and Z.S.; visualization, H.T., R.L., X.L., Y.W. (Yaqian Wang), Y.W. (Yiyang Wu), Y.W. (Yu Wu) and Z.S.; supervision, Y.W. (Yunfeng Wang); project administration, Y.W. (Yunfeng Wang); funding acquisition, M.L. All authors have read and agreed to the published version of the manuscript.

Funding: This work was supported by the National Natural Science Foundation of China (NSFC) under Grants 71531011, 71771048, 71432007, 71832001, 71871159, and 71571134.

Data Availability Statement: The data that support the findings of this study are available from the corresponding author upon reasonable request.

Acknowledgments: We sincerely thank the editor and anonymous reviewers for their valuable suggestions! We would also like to thank Zhanguo Zhu for his constructive comments and valuable suggestions!

Conflicts of Interest: The authors declare no conflict of interest.

References

1. Tendall, D.M.; Joerin, J.; Kopainsky, B.; Edwards, P.; Shreck, A.; Le, Q.B.; Krütli, P.; Grant, M.; Six, J. Food system resilience: Defining the concept. *Glob. Food Secur.* **2015**, *6*, 17–23. [\[CrossRef\]](#)
2. Love, D.C.; Allison, E.H.; Asche, F.; Belton, B.; Cottrell, R.S.; Froehlich, H.E.; Gephart, J.A.; Hicks, C.C.; Little, D.C.; Nussbaumer, E.M.; et al. Emerging COVID-19 impacts, responses, and lessons for building resilience in the seafood system. *Glob. Food Secur.* **2021**, *28*, 100494. [\[CrossRef\]](#) [\[PubMed\]](#)
3. Headey, D. Rethinking the global food crisis: The role of trade shocks. *Food Policy* **2011**, *36*, 136–146. [\[CrossRef\]](#)
4. Ivanov, D.; Dolgui, A. OR-methods for coping with the ripple effect in supply chains during COVID-19 pandemic: Managerial insights and research implications. *Int. J. Prod. Econ.* **2021**, *232*, 107921. [\[CrossRef\]](#)
5. Hosseini, S.; Ivanov, D. A multi-layer Bayesian network method for supply chain disruption modelling in the wake of the COVID-19 pandemic. *Int. J. Prod. Res.* **2021**, *60*, 5258–5276. [\[CrossRef\]](#)
6. Ivanov, D. Exiting the COVID-19 pandemic: After-shock risks and avoidance of disruption tails in supply chains. *Ann. Oper. Res.* **2021**, *1–18*. [\[CrossRef\]](#)
7. Liu, M.; Liu, Z.; Chu, F.; Zheng, F.; Chu, C. A new robust dynamic Bayesian network approach for disruption risk assessment under the supply chain ripple effect. *Int. J. Prod. Res.* **2021**, *59*, 265–285. [\[CrossRef\]](#)
8. Davis, K.F.; Downs, S.; Gephart, J.A. Towards food supply chain resilience to environmental shocks. *Nat. Food* **2021**, *2*, 54–65. [\[CrossRef\]](#)
9. Hobbs, J.E. Food supply chain resilience and the COVID-19 pandemic: What have we learned? *Can. J. Agric. Econ. Can. D'Agroecon.* **2021**, *69*, 189–196. [\[CrossRef\]](#)
10. Sawik, T. Disruption mitigation and recovery in supply chains using portfolio approach. *Omega* **2019**, *84*, 232–248. [\[CrossRef\]](#)
11. Sawik, T. Stochastic Optimization of Supply Chain Resilience under Ripple Effect: A COVID-19 Pandemic Related Study. *Omega* **2022**, *109*, 102596. [\[CrossRef\]](#)
12. Freeman, N.; Mittenthal, J.; Keskin, B.; Melouk, S. Sourcing strategies for a capacitated firm subject to supply and demand uncertainty. *Omega* **2018**, *77*, 127–142. [\[CrossRef\]](#)
13. He, J.; Alavifard, F.; Ivanov, D.; Jahani, H. A real-option approach to mitigate disruption risk in the supply chain. *Omega* **2019**, *88*, 133–149. [\[CrossRef\]](#)
14. Rezapour, S.; Farahani, R.Z.; Pourakbar, M. Resilient supply chain network design under competition: A case study. *Eur. J. Oper. Res.* **2017**, *259*, 1017–1035. [\[CrossRef\]](#)
15. Liu, M.; Liu, Z.; Chu, F.; Dolgui, A.; Chu, C.; Zheng, F. An optimization approach for multi-echelon supply chain viability with disruption risk minimization. *Omega* **2022**, *112*, 102683. [\[CrossRef\]](#)
16. Sawik, T. Selection of resilient supply portfolio under disruption risks. *Omega* **2013**, *41*, 259–269. [\[CrossRef\]](#)
17. Sawik, T. On the risk-averse selection of resilient multi-tier supply portfolio. *Omega* **2021**, *101*, 102267. [\[CrossRef\]](#)
18. Lückner, F.; Seifert, R.W.; Biçer, I. Roles of inventory and reserve capacity in mitigating supply chain disruption risk. *Int. J. Prod. Res.* **2019**, *57*, 1238–1249. [\[CrossRef\]](#)
19. Moretto, A.; Patrucco, A.S.; Harland, C.M. The dynamics of reshoring decisions and the role of purchasing. *Int. J. Prod. Res.* **2020**, *58*, 5929–5944. [\[CrossRef\]](#)
20. Azad, N.; Saharidis, G.K.; Davoudpour, H.; Malekly, H.; Yektamaram, S.A. Strategies for protecting supply chain networks against facility and transportation disruptions: An improved Benders decomposition approach. *Ann. Oper. Res.* **2013**, *210*, 125–163. [\[CrossRef\]](#)
21. Gholami-Zanjani, S.M.; Jabalameli, M.S.; Klibi, W.; Pishvae, M.S. A robust location-inventory model for food supply chains operating under disruptions with ripple effects. *Int. J. Prod. Res.* **2021**, *59*, 301–324. [\[CrossRef\]](#)
22. Gholami-Zanjani, S.M.; Jabalameli, M.S.; Pishvae, M.S. A resilient-green model for multi-echelon meat supply chain planning. *Comput. Ind. Eng.* **2021**, *152*, 107018. [\[CrossRef\]](#)
23. Gholami-Zanjani, S.M.; Klibi, W.; Jabalameli, M.S.; Pishvae, M.S. The design of resilient food supply chain networks prone to epidemic disruptions. *Int. J. Prod. Econ.* **2021**, *233*, 108001. [\[CrossRef\]](#)
24. Ivanov, D.; Rozhkov, M. Disruption Tails and Revival Policies in the Supply Chain. In *Handbook of Ripple Effects in the Supply Chain*; Springer: Berlin/Heidelberg, Germany, 2019; pp. 229–260.
25. Burgos, D.; Ivanov, D. Food retail supply chain resilience and the COVID-19 pandemic: A digital twin-based impact analysis and improvement directions. *Transp. Res. Part E Logist. Transp. Rev.* **2021**, *152*, 102412. [\[CrossRef\]](#)
26. Shen, Z.M.; Sun, Y. Strengthening supply chain resilience during COVID-19: A case study of JD.com. *J. Oper. Manag.* **2021**. [\[CrossRef\]](#)

27. Barandun, G.; Soprani, M.; Naficy, S.; Grell, M.; Kasimatis, M.; Chiu, K.L.; Ponzoni, A.; Güder, F. Cellulose fibers enable near-zero-cost electrical sensing of water-soluble gases. *ACS Sens.* **2019**, *4*, 1662–1669. [[CrossRef](#)]
28. Guo, L.; Wang, T.; Wu, Z.; Wang, J.; Wang, M.; Cui, Z.; Ji, S.; Cai, J.; Xu, C.; Chen, X. Portable Food-Freshness Prediction Platform Based on Colorimetric Barcode Combinatorics and Deep Convolutional Neural Networks. *Adv. Mater.* **2020**, *32*, 2004805. [[CrossRef](#)]
29. Ivanov, D.; Dolgui, A. A digital supply chain twin for managing the disruption risks and resilience in the era of Industry 4.0. *Prod. Plan. Control* **2021**, *32*, 775–788. [[CrossRef](#)]
30. Fescioglu-Unver, N.; Choi, S.H.; Sheen, D.; Kumara, S. RFID in production and service systems: Technology, applications and issues. *Inf. Syst. Front.* **2015**, *17*, 1369–1380. [[CrossRef](#)]
31. Bag, A.; Lee, N.E. Recent advancements in development of wearable gas sensors. *Adv. Mater. Technol.* **2021**, *6*, 2000883. [[CrossRef](#)]
32. Bhagya Raj, G.; Dash, K.K. Comprehensive study on applications of artificial neural network in food process modeling. *Crit. Rev. Food Sci. Nutr.* **2022**, *62*, 2756–2783. [[CrossRef](#)] [[PubMed](#)]
33. Zahiri, B.; Zhuang, J.; Mohammadi, M. Toward an integrated sustainable-resilient supply chain: A pharmaceutical case study. *Transp. Res. Part E Logist. Transp. Rev.* **2017**, *103*, 109–142. [[CrossRef](#)]
34. Abbasi, S.; Saboury, A.; Jabalameli, M.S. Reliable supply chain network design for 3PL providers using consolidation hubs under disruption risks considering product perishability: An application to a pharmaceutical distribution network. *Comput. Ind. Eng.* **2021**, *152*, 107019. [[CrossRef](#)]
35. Diabat, A.; Jabbarzadeh, A.; Khosrojerdi, A. A perishable product supply chain network design problem with reliability and disruption considerations. *Int. J. Prod. Econ.* **2019**, *212*, 125–138. [[CrossRef](#)]
36. Yavari, M.; Zaker, H. Designing a resilient-green closed loop supply chain network for perishable products by considering disruption in both supply chain and power networks. *Comput. Chem. Eng.* **2020**, *134*, 106680. [[CrossRef](#)]
37. Dolgui, A.; Tiwari, M.K.; Sinjana, Y.; Kumar, S.K.; Son, Y.J. Optimising integrated inventory policy for perishable items in a multi-stage supply chain. *Int. J. Prod. Res.* **2018**, *56*, 902–925. [[CrossRef](#)]
38. Laporte, G.; Louveaux, F.V. The integer L-shaped method for stochastic integer programs with complete recourse. *Oper. Res. Lett.* **1993**, *13*, 133–142. [[CrossRef](#)]
39. Angulo, G.; Ahmed, S.; Dey, S.S. Improving the integer L-shaped method. *INFORMS J. Comput.* **2016**, *28*, 483–499. [[CrossRef](#)]
40. Liu, M.; Wang, S.; Chu, C.; Chu, F. An improved exact algorithm for single-machine scheduling to minimise the number of tardy jobs with periodic maintenance. *Int. J. Prod. Res.* **2016**, *54*, 3591–3602. [[CrossRef](#)]
41. Van Slyke, R.M.; Wets, R. L-shaped linear programs with applications to optimal control and stochastic programming. *SIAM J. Appl. Math.* **1969**, *17*, 638–663. [[CrossRef](#)]

Disclaimer/Publisher’s Note: The statements, opinions and data contained in all publications are solely those of the individual author(s) and contributor(s) and not of MDPI and/or the editor(s). MDPI and/or the editor(s) disclaim responsibility for any injury to people or property resulting from any ideas, methods, instructions or products referred to in the content.